

Beam-Target helicity asymmetry in charged pion photo-production from polarized neutrons in solid HD using the CLAS at Jefferson Lab

T. Kageya¹, D. Ho², P. Peng³, F. Klein⁴, A.M. Sandorfi¹, and R. Schumacher²

¹*Thomas Jefferson National Accelerator Facility, Newport News, VA 23606, USA*

²*Carnegie Mellon University, Pittsburgh, PA 15213, USA*

³*University of Virginia, Charlottesville, VA 22903 USA and*

⁴*George Washington University, Washington, DC 20052, USA*

(for the CLAS Collaboration)

(Dated: December 22, 2016)

Single charged-pion photoproduction from circularly polarized photons and longitudinally-polarized deuterons has been measured in the CLAS detector at Jefferson Lab. Preliminary E asymmetries for the exclusive reaction, $\gamma + n(p) \rightarrow \pi^- + p(p)$, have been extracted with three very different methods and are in excellent agreement. These data are expected to provide significant new constraints on photoproduction multipoles from the neutron for which data is sparse.

I. INTRODUCTION

The E06-101 (g14) experiment was performed in Hall B of the Thomas Jefferson National Accelerator Facility (Jlab), during the period from December 2012 to May 2013. Data included in the present analysis were taken with circularly polarized photon beams whose energy ranged from 0.85 to 2.4 GeV, yielding 4.1×10^9 trigger events.

Frozen-spin Deuterium-Hydride (HD) targets [1, 2] were used to provide longitudinally polarized quasi-free neutrons. The HD In-Beam Cryostat (IBC) [1] operated as a dilution refrigerator and maintained targets at 50 mK in an 0.9 T superconducting solenoid. The target polarizations were calibrated in a separate production dewar and monitored by NMR in the IBC. Average Deuteron polarizations were about 26% during experiments and the relaxation time for the deuteron polarization was measured to be more than a year for the run periods in this analysis.

Three different analysis techniques have been applied to the data to extract the E asymmetries: (A) conventional background suppression via sequential requirements (cuts) and empty-cell subtraction, and advanced statistical methods that employed (B) kinematic fitting and (C) a Boosted Decision Tree (BDT) algorithm. These are compared and combined in the subsequent sections.

II. DATA REDUCTION

Circularly polarized gamma-ray beams were produced by the bremsstrahlung of electrons that were longitudinally polarized (typically to 85%). Photon energies were defined by the detection of the post-bremsstrahlung electrons in a tagging spectrometer. This analysis focused on the $\pi^- +$ proton final state, with particles detected in the CEBAF Large Acceptance Spectrometer (CLAS). Multiple reaction channels were used to calibrate both

the tagging spectrometer and the CLAS detector.

In each of the three analysis methods, a π^- and a proton were identified using the correlation between velocity, calculated from time of flight (TOF), and particle momentum, as measured by drift chamber within the CLAS torus magnetic field. The selection was restricted to events in which only one π^- and one proton were detected. Corrections were made for the energy losses of the charged particles as they emerged from the target material and traversed the CLAS detector.

To select quasi-free neutrons, each analysis also restricted events to those with a missing momentum for an undetected proton from the $\gamma + n(p) \rightarrow \pi^- + p(p)$ reaction of ≤ 0.1 GeV. (Tighter restrictions had no significant effect on the extracted asymmetries.)

Tracking of the charged particles in the CLAS drift chambers allowed a reconstruction of the reaction vertex. The result for full and empty target cells are shown in Figure 1. The arrows indicate the regions included in the different analyses.

A. Background subtraction

Here a sequence of cuts is applied to isolate the final state. Since in the quasi-free limit the desired reaction is 2-body, events in which azimuthal angle difference between the proton and the π^- is within 180 ± 20 degrees are selected.

The square of the missing mass of a spectator proton is constructed for the reaction, $\gamma + D \rightarrow \pi^- + p + X$ and events are selected for which that value is below 1.1 GeV².

The background contribution from the pCTFE target cell windows and thin Aluminum cooling wires [1] is obtained from data taken with an empty target cell, scaled to the same photon flux, imposing analysis requirements identical to the full target data [3]. The contributions to the yields from the target cell windows are thus removed by subtraction. This process is carried out independently

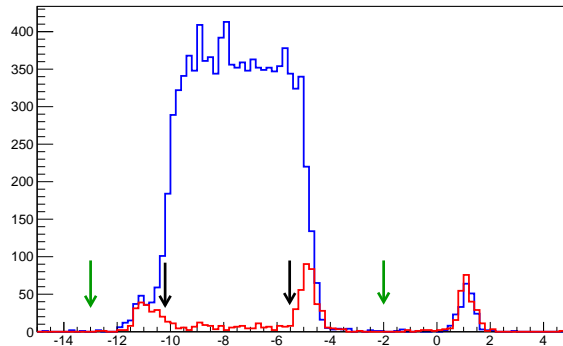


FIG. 1. The reaction vertex for a sample of data, reconstructed along the beam axis with the horizontal scale in cm, is shown for full (blue) and empty (red) target cells, normalized to the same photon flux. (The peak centered near +1 cm is generated by a foil within the cryostat and is independent of the target.) The arrows bound the regions included in the (A) Background subtraction (green arrows), and (B) and (C) advanced statistical analyses (black arrows).

for every angle and energy bin.

B. Kinematic fitting

Kinematic fitting (KinFit) uses the constraints of energy and momentum conservation to improve the accuracy of measured quantities, and so obtain improved estimates on the momenta of undetected particles [4]. This allows a natural separation of reactions with additional particles in the final state, as well as reactions on bound nucleons in the target cell material, since these do not strictly follow elementary kinematics. In this analysis, a pre-selection of events eliminated the target cell windows with cuts on the vertex reconstruction (Figure 1), leaving only the background from aluminum cooling wires to be removed by the fitting algorithm. Kinematic fitting also emphasizes quasi-free reactions by significantly suppressing contributions from high-momentum neutrons in the deuteron.

For each event, a confidence level is calculated, assuming the reaction $\gamma + (n) \rightarrow \pi^- + p$, where the target is assumed to have the neutron mass but unknown momentum [5]. On this confidence level distribution a requirement of ≥ 0.05 has been applied to extract the reaction yields. This confidence level requirement was varied to investigate the impact on the extracted asymmetries (1.3 % relative) and the results of this and similar systematic studies are summarized in Table I.

C. Boosted Decision Trees

When viewing exclusive events in a quasi- 4π detector such as the CLAS, many different kinematic variables can be constructed. Conventional analyses, such as discussed in (A) above, view each of these in different projected low-level dimensions and place sequential cuts on

the data to extract the reaction of interest. In contrast, multivariate *Boosted Decision Trees* (BDT) can be used to view each event in a higher dimension where all cuts can be placed *simultaneously* [6, 7]. The process creates a *forest* of logical *if-else* tests for every kinematic variable and the resulting decision trees are applied to all of the available information.

In this application, $\pi^- + p$ candidate events were pre-selected with requirements on their TOF and CLAS momenta, and their reconstructed vertex was required to lie within the region excluding the target cell windows (within the black arrows of Figure 1). The BDT algorithm was *trained* on a Monte Carlo of the CLAS response to the reaction of interest and on the empty target data, and then used to separate each event into either *signal* or *background* [8]. This procedure retained an average of 40% more $\pi^- + p$ events, which resulted in smaller statistical errors, and yielded asymmetry results in good agreement with the other analysis methods. Parameters of the procedure were varied to study the associated systematic uncertainties, and these are summarized in Table I.

III. PRELIMINARY RESULTS

The asymmetries resulting from the three analysis methods are statistically consistent. As an example, E asymmetries as a function of $\cos \theta_{\pi^-}$, calculated in the center of mass of the $\gamma+n$ system, are shown in Figure 2 for each of the three analysis methods at a sample of four different energies, $W = 1.50, 1.78, 2.06$ and 2.22 GeV. The magenta, red and blue points are results from the *Background Subtraction*, *kinematic fitting* and *BDT* analyses, respectively.

A weighted average of the results from the three analyses has been used to give the best estimate of the E asymmetries. In calculating the net error, we have used

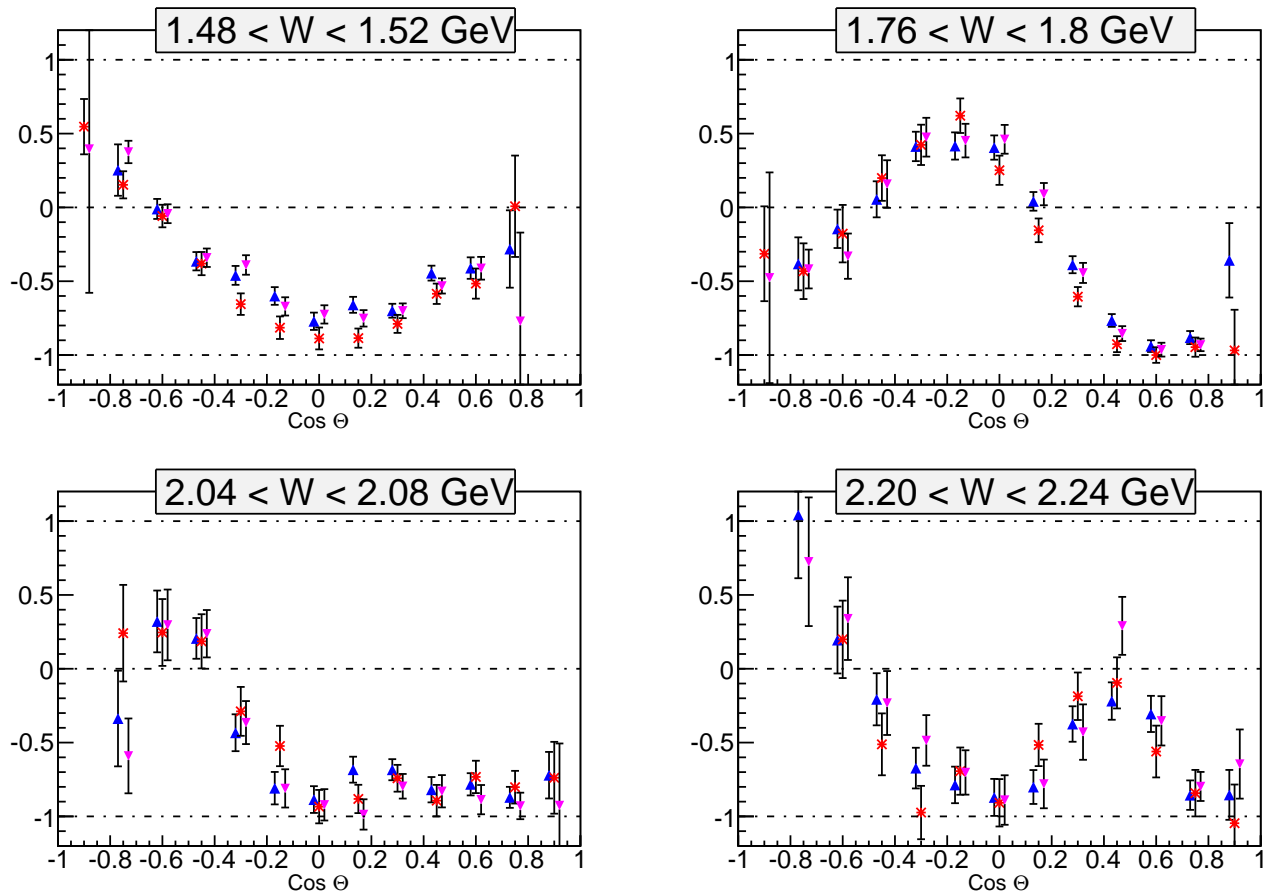


FIG. 2. Preliminary E asymmetries are plotted as a function of $\cos \theta_{\pi^-}$ in the $\gamma+n$ CM frame from the three analysis methods (Magenta: *Background Subtraction*; Red: *kinematic fitting*; Blue: *BDT*) for (a) $1.48 \leq W \leq 1.52$ GeV, (b) $1.76 \leq W \leq 1.8$ GeV, (c) $2.04 \leq W \leq 2.08$ GeV and (d) $2.20 \leq W \leq 2.24$ GeV.

standard methods to estimate the correlations between the analyses [9], which are only partial since the different analysis requirements result in a selection of different sets of events. The resulting asymmetries are shown in Figure 3, for a sample of twelve W bins, ranging from 1.52 to 2.28 GeV. Also plotted there are predictions from Partial Wave Analyses (PWA) by the George Washington University *SAID* group (red curves) [10] and the Bonn-Gatchina (BoGn) collaboration (black curves) [11]. The predictions are largely consistent with the asymmetry data at lower energies, but significant deviations develop with increasing energy. This is to be expected since photo-production data from the neutron is quite limited and the production amplitude is under-constrained. New

PWA which include fits to these data are now underway and will undoubtedly lead to significant modifications to the neutron multipoles.

Systematic variations to the data have been studied by changing parameter values for each of the three analysis methods and the results are summarized in Table I. The systematic uncertainty associated with analysis and event processing enter the three methods in different ways, but total about 4% in each case. Nonetheless, the systematic polarization error dominates (6.9%) and leads to a total systematic uncertainty of 8% for the experiment.

This work was supported by the U.S. Department of Energy, Office of Science, Office of Nuclear Physics under contract DE-AC05-06OR23177.

- [1] C.D. Bass, *et al.*, Nucl. Inst. Meth. Phys. Res. **A737**, 107 (2014).
 [2] M.M. Lowry, *et al.*, Nucl. Inst. Meth. Phys. Res. **A815**, 31 (2016).

- [3] T. Kageya *et al.*, Int. J. Mod. Phys. Conf. Ser. **26** (2014) 1460079.
 [4] A.G. Frodesen and O. Skjeggstad, *Probability and Statistics in Particle Physics*, Universitetsforlaget,

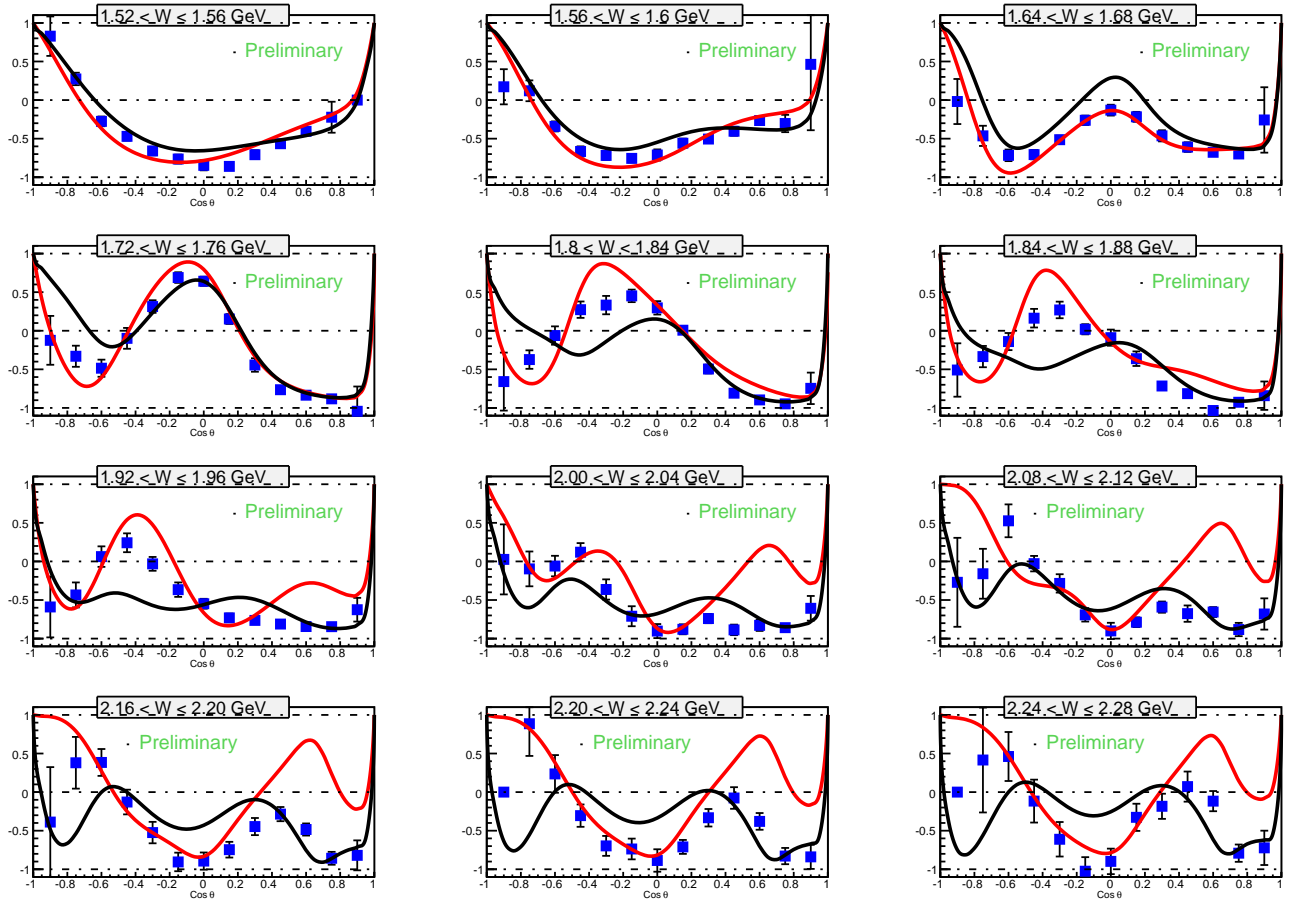


FIG. 3. Net exclusive E asymmetries, as a function of $\cos \theta_{\pi^-}$ in the $\gamma+n$ CM frame, for a sample of twelve W ranges from 1.52 to 2.28 GeV (bottom left). Only statistical errors are shown. Two PWA analysis predictions are plotted for SAID[solution CM12] [10](red curves) and BoGn[solution 2011-02] [11](black curves).

Bergen, Norway (1979); ISBN 82-00-01906-3.

- [5] Peng Peng, *Polarization observables for single and double charged pion photo-production with polarized HD target*, Ph.D. thesis, University of Virginia (2015).
- [6] H. Drucker and C. Cortes, *Adv. Neural Inform. Process Sys.* **8** (1996).
- [7] A. Hoecker, *et al.*, arXiv:physics/0703039.
- [8] Ph.D thesis by Dao Ho, *Measurements of the E Polarization Observable for $\gamma D \rightarrow \pi^- p(p_s)$, ...*, Ph.D. thesis, Carnegie-Mellon University (2015).
- [9] M. Schmelling, *Physics Scripta.* **51**, 676 (1995).
- [10] R.L. Workman, *et al.*, *Phys. Rev C***86**, 015202 (2012).
- [11] A.V. Anisovich *et al.*, *Eur. Phys J. A***48**, 15 (2012).

TABLE I. Estimated systematic errors for each of the three analysis methods, and for beam and target polarization. (All errors are relative.)

Contribution to σ_{sys}	σ_{sys}		
	BkgSub	KinFit	BDT
z-vertex cut / Kel-F suppression:	2.6%	1.4%	1.7%
Confidence level cut / BDT cut:		1.3%	0.7%
Missing momentum cut:	1.7%	2.9%	1.4%
PID cut:	1.3%		
Missing mass cut:	1.4%		2.6%
Coplanarity cut:	0.4%		
Monte Carlo (DC resolution):			0.4%
Extrapolation to $ \vec{p}_{miss} =0$:	2.2%	2.2%	2.2%
σ_{sys} (cuts):	4.2%	3.9%	4.3%
Photon beam polarization:	3.4%	3.4%	3.4%
Target polarization:	6.0%	6.0%	6.0%
σ_{sys} (polarization):	6.9%	6.9%	6.9%
σ_{sys} (total):	8.0%	7.9%	8.1%